Desalination 510 (2021) 115089

Contents lists available at ScienceDirect

Desalination

journal homepage: www.elsevier.com/locate/desal

Correlation equation for evaluating energy consumption and process performance of brackish water desalination by electrodialysis

Li Wang, Sohum K. Patel, Menachem Elimelech *

[a] Department of Chemical and Environmental Engineering, Yale University, New Haven, CT 06520-8286, USA
[b] Nanosystems Engineering Research Center for Nanotechnology-Enabled Water Treatment (NEWT), Yale University, USA

HIGHLIGHTS

- Derived correlation equation for predicting energy consumption of electrodialysis
- Demonstrated robustness of correlation equation as compared to ion transport model
- Correlation equation reliably predicted literature reported energy consumption data
- Utilized correlation equation as a simple yet powerful performance analysis tool

GRAPHICAL ABSTRACT

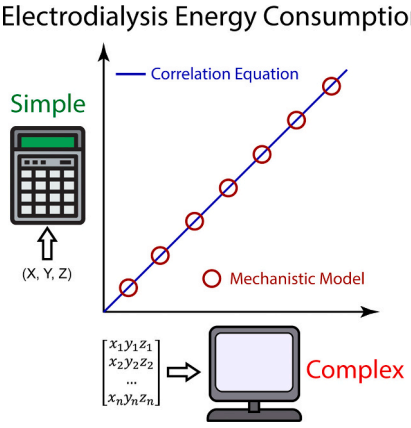

ARTICLE INFO

Keywords:
Electrodialysis
Brackish water desalination
Energy consumption
Performance analysis
Correlation equation

ABSTRACT

Electrodialysis (ED) is an electro-driven desalination technology that relies on the selective transport of ions through ion exchange membranes. Though several approaches have been developed to model and evaluate the performance of ED, mechanistic ion-transport models, which rigorously solve the fundamental Nernst-Planck equation, remain some of the most reliable and utilized. However, complexity of the involved transport phenomena prevents analytical solutions of such models, and numerical solutions can be prohibitively intensive. Here, we use an equivalent circuit analogue to derive a simple correlation equation that predicts the energetic performance of ED for brackish water desalination. Specifically, our correlation equation predicts the specific energy consumption of ED for a given productivity, set of desalination parameters (i.e., feed salinity, salt removal, water recovery), and system properties. The correlation equation demonstrates robustness in predicting the specific energy consumption across a wide range of operational parameters, showing excellent agreement with a Nernst-Planck ion-transport model and literature-reported experimental data. Furthermore, we use the developed correlation equation to show the dependence of the specific energy consumption on the productivity, highlighting the tradeoff between the thermodynamic energy efficiency and desalination rate of the ED process.

* Corresponding author.
E-mail address: menachem.elimelech@yale.edu (M. Elimelech).

https://doi.org/10.1016/j.desal.2021.115089
Received 21 February 2021; Received in revised form 8 April 2021; Accepted 8 April 2021
Available online 21 April 2021

Overall, our developed correlation equation provides a convenient alternative to computationally intensive mechanistic models for performance analysis of the ED process.

Nomenclature

AEM	Anion Exchange Membrane
CEM	Cation Exchange Membrane
ED	Electrodialysis
IEM	Ion Exchange Membrane
SEC_{min}	Minimum Specific Energy Consumption
SEC	Specific Energy Consumption
TEE	Thermodynamic Energy Efficiency
WR	Water Recovery

Symbol

A_m	Membrane area
c	Salt concentration
c_0	Feed salinity
c_b	Brine salinity
c_d	Diluate salinity
$c_{T,\,m}$	Total ion concentration in IEM
D_d	Effective diffusion coefficient
D_e	Effective diffusion coefficient for electromigration
D_m	Diffusion coefficient in IEM
F	Faraday constant
J	Ion flux
J_{ion}	Total ion flux
j_{st}	Salt loading parameter
$\bar{I}$	Spatially averaged current
L_{sp}	Spacer channel thickness
P	Productivity
q	Transferred charge
$Q_{b,r}$	Volumetric flowrate of the recirculated brine stream
$Q_{b,f}$	Volumetric flowrate of the "makeup" feed stream to the brine channels
Q_d	Volumetric flowrate of the diluate stream
R	ED stack resistance
R_g	Gas constant
S	IEM selectivity
S_p	Selectivity parameter
S_r	Salt removal
T	Absolute temperature
t_d	Desalination duration
V	Cell pair voltage
v	Flow velocity
V_t	Thermal voltage
X	IEM fixed charge density
z_i	Charge of ion i

Greek letter

ϕ	Dimensionless electrical potential
ϕ_m	Dimensionless electrical potential in IEM
ω	Sign of fixed charge group in IEM

1. Introduction

Affecting over two-thirds of the world population at least one month per year [1], global water scarcity poses as a primary obstacle towards sustained economic and societal development. With the planet's already scarce freshwater sources being depleted and polluted, the desalination of unconventional water sources is essential to combat water scarcity. Accordingly, the number of operational desalination plants has doubled over just the last two decades, with such large growth rates in the global desalination capacity expected to continue. Recently, electro-driven desalination processes have increasingly been considered as potential alternatives to mature technologies such as reverse osmosis and thermal distillation [2–5]. Among the electro-driven technologies, electrodialysis (ED) is the most established and has gained renewed interest due to its high energy efficiency, low propensity to fouling, tunability of salt removal, facile scalability, and high water recovery [6–10].

The underlying principle of ED is to remove salt from saline feedwater by transporting the ions in solution through ion exchange membranes (IEMs) under the influence of an electrical field. A unit cell of ED consists of two types of IEMs — a cation exchange membrane (CEM) and an anion exchange membrane (AEM) — which allow for the selective passage of cations and anions, respectively. In practice, numerous unit cells are arranged in alternating fashion to make up an ED stack, across which an external voltage is applied to generate an ionic current through the IEMs. After the ions migrate through one type of IEM, they are blocked from crossing the following IEM, thus producing diluate and brine streams from the feedwater.

Though ED is a mature desalination technology, which has been applied to many full-scale applications since the 1970's, the process has continued to develop through a multitude of research directions. For example, recently, researchers have investigated the application of monovalent-selective IEMs in ED to achieve selective separation of monovalent ions from multivalent ions [11,12]. Extensive research has also been directed towards the development of improved IEMs, in terms of their selectivity, electrical resistance, and cost [13–15]. Furthermore, efforts have been aimed at demonstrating the compatibility of ED with sustainable energy sources, such as solar or wind power [16,17].

With ED already being widely employed for brackish water desalination and interest in the process growing, prediction and optimization of process performance is of paramount importance. Several theoretical studies have investigated the effects of operation conditions (e.g., flowrate, cell voltage, flowrate split ratio) on ED performance [18–21]. However, mechanistic modeling of the ion transport phenomena in ED is complex. Specifically, ion transport in ED involves advective transport in the direction of water flow (i.e., parallel to IEMs), as well as electromigration and diffusion through the IEMs (i.e., perpendicular to IEMs) [22–24]. Further complicating the modeling of ED is the non-ideal selectivity of IEMs, by which counterion transport across the membranes is accompanied by some degree of co-ion leakage [7,25]. Also, as the ions permeate through the IEMs, the salt concentration in the proximity of the membranes diverges from that in the bulk solution (typically termed concentration polarization), thus influencing ion transport through the membranes [26,27]. Rigorous consideration of such phenomena makes analytical approaches prohibitively difficult and numerical solutions computationally intensive [22,23,28,29].

The variety of operational parameters in ED introduces another dimension of difficulty in modeling and evaluating process performance. At present, most process investigation focuses solely on evaluating the effects of operation conditions on the energy consumption and diluate concentration. A comprehensive performance analysis of ED, however, must consider both the energy consumption and desalination rate for a targeted separation (i.e., feed concentration, effluent concentration, and

Table 1
Summary of the parameters of the correlation equation.

Parameter	Physical interpretation	Units
c_0	Feed concentration	mol m^{-3}
c_b	Brine concentration	mol m^{-3}
c_d	Diluate concentration	mol m^{-3}
L_{sp}	Thickness of the spacer channel	m
j_{st}	Salt loading as defined by Eq. (15)	mol m^{-2}
P	Productivity	L m^{-2} h^{-1}
S_r	Salt rejection as defined by Eq. (5)	
X	Volumetric fixed charge density of ion exchange membrane	mol m^{-3}

Table 2
Specified parameters and respective range of values used in the mechanistic model for development of the correlation equation.

Parameter	Range
c_0	17.1–171 mol m^{-3}
P	20–78 L m^{-2} h^{-1}
S_r	0.1–0.9
WR	0.5–0.9
X	3000–6000 mol m^{-3}

Table 3
Summary of the fitting coefficients in the correlation equation (Eq. (20)).

Coefficient	Value
α	0.517
β	−0.966
γ	0.281
C	0.091
m	0.44

water recovery), as has been demonstrated for other desalination technologies [30–32]. In ED, the rate of desalination, otherwise referred to as productivity, is generally controlled by adjusting the volumetric flow rate through the spacer channels. However, the flow rate influences several other transport phenomena in ED (e.g., concentration polarization and advective transport parallel to IEMs), making such analysis nontrivial and requiring the use of a rigorous mechanistic model. With no facile method for ED process optimization currently available, the development of a mathematically simple, yet accurate approach is critical.

In this study, we develop a correlation equation capable of reliably predicting the specific energy consumption (*SEC*) of desalination by ED across a broad range of brackish water conditions. We begin by identifying the key performance metrics (*SEC* and productivity), separation parameters, and system properties necessary for evaluating the electrodialysis process. To ensure our correlation equation is both easily accessible and physically intuitive, we utilize a simple electrical circuit analogue to represent the fundamental mechanisms of ED. Ultimately, we derive a power law relation which relates the *SEC* to the productivity and two newly defined surrogate parameters — salt loading and membrane selectivity — which consider the separation conditions and key system properties. We capture the effects of complex transport phenomena, such as co-ion transport and concentration polarization, by fitting the correlation equation coefficients with the results of a rigorous two-dimensional Nernst-Planck ion transport model. After developing the correlation equation, we demonstrate its excellent agreement with the ion transport model and literature data, and end by highlighting its utility as a performance analysis tool.

2. Electrodialysis performance metrics and desalination parameters

2.1. ED process operation

In this study, we consider a 50-cell pair ED stack, with each cell pair consisting of an AEM, CEM, concentrate channel, and diluate channel. The stack is operated using single-pass continuous flow, and assumed to be at steady state conditions. The cell pairs are situated between a pair of electrodes, which upon being polarized, induce the transport of ions in the flow channels towards the oppositely polarized electrode. Cations readily pass through the CEMs, while anions selectively cross the AEMs.

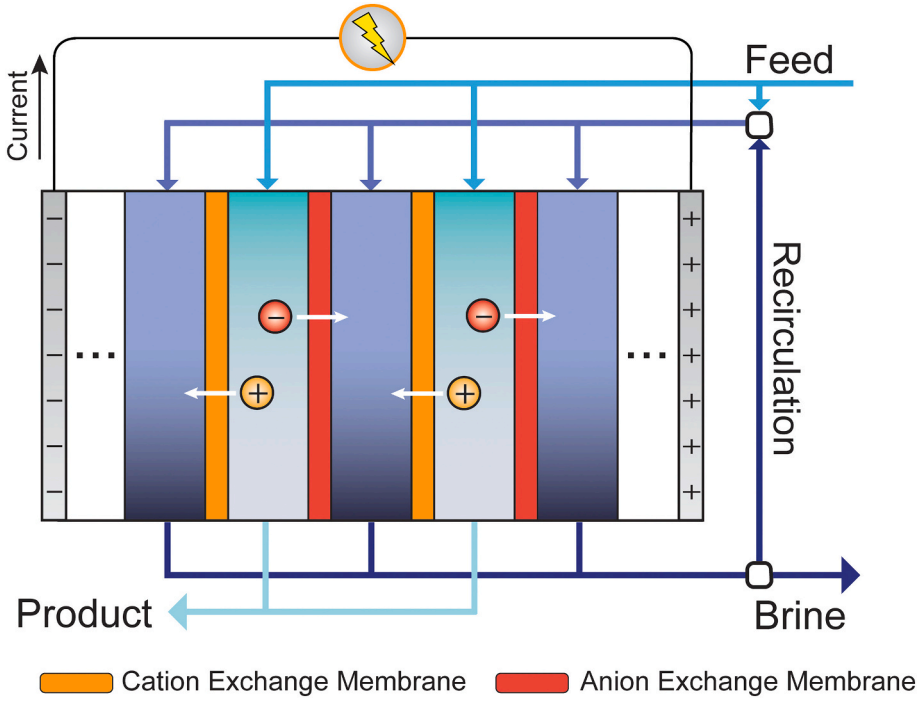

Fig. 1. Schematic illustration of the electrodialysis process operated in feed-and-bleed mode. Upon applying an external voltage across the electrodes at the ends of the ED stack, cations and anions in the flow channels migrate in opposite directions according to the electric field. Cations and anions cross the cation exchange membrane (CEM) and anion exchange membrane (AEM), respectively, while being blocked from passing through the alternate membrane. Thus, diluate and concentrate streams are alternatively produced across the stack. The ionic current passing through the ED stack is converted into an electrical current via redox reactions at the electrodes. In the feed-and-bleed mode, a fraction of the brine stream is recirculated and mixed with the feedwater entering the concentrate channels. Adjusting the fraction of brine which is recirculated allows for control of the system-scale water recovery, while maintaining equal flowrate through the diluate and concentrate channels.

Such transport, termed counter-ion flux, results in desalination of the feedwater in the diluate channels, while generating brine in the concentrate channels. However, the IEMs are not perfectly selective in their rejection of ions with the same charge. Thus, some degree of co-ion transport, which compromises the efficiency of ED desalination, is also permitted. Throughout our study, we only consider a 1:1 monovalent salt, with the diffusion coefficients being based on NaCl.

The extent of desalination is controlled by varying the applied voltage between the electrodes, with larger voltages producing greater current densities and degrees of salt removal. Though the salt removal can readily be manipulated in ED by altering the electric driving force, the water recovery — the volume of product water generated per volume of feedwater — is more difficult to control. As is typical of practical ED operation, the flowrate in adjacent flow channels is held equal to mitigate convective water transport across the IEMs, thereby fixing the module-scale water recovery at 50% [33]. Therefore, to increase the system-scale water recovery (*WR*), we employ feed-and-bleed operation, by which a portion of the brine exiting the ED stack is recirculated and fed back to the concentrate flow channels [34,35]. In effect, the overall volume of feedwater which must be supplied to the concentrate channels for a given volume of product water is reduced. We note that when operating at high water recoveries in feed-and-bleed operation, the salinity of the concentrate can become significantly higher than that of the diluate, with these large concentration gradients increasing the energy demand for a given separation.

2.2. Performance metrics

In the evaluation of desalination processes, two metrics are critical: the energy consumption and the productivity (i.e., desalination rate normalized by projected membrane area). The energy consumption is related to the operational cost of desalination, while the productivity determines the required system size (or membrane area) and is thereby indicative of capital cost. Throughout the analysis, we focus on a single-pass continuous flow ED system at steady state conditions.

To measure the energy consumption, the specific energy consumption (*SEC*) is commonly adopted, which is defined as the energy consumed to produce a unit volume of diluate water. The *SEC* for ED is thus expressed as

$$SEC = \frac{V\bar{I}}{Q_d} \tag{1}$$

where V is the cell pair voltage, $\bar{I}$ is the spatially averaged current, and Q_d is the volumetric flowrate of the diluate (product) stream through a single flow channel. Note that though Eq. (1) is based on a single cell pair, the value of *SEC* for the entire stack is the same since both V and Q_d are directly proportional to the number of cell pairs. Also, the potential drops associated with the redox reactions occurring at the electrodes are neglected, as their contribution to the overall stack voltage, and thus the *SEC*, is insignificant for a typical stack consisting of numerous cell pairs. At steady state, the current does not change with time, though it varies along the longitudinal direction (flow direction) of the ED cell. To keep the calculation of *SEC* simplified, the spatially averaged current ($\bar{I}$) is utilized in Eq. (1).

A relevant metric to gauge the relative energy consumption of a desalination process is the thermodynamic energy efficiency (*TEE*), which is the ratio of the minimum specific energy consumption of separation (SEC_{min}) and the practical *SEC*:

$$TEE = \frac{SEC_{min}}{SEC} \tag{2}$$

The SEC_{min} is the energy consumed to achieve a separation in a thermodynamically reversible manner and is determined by [36]

$$SEC_{min} = 2R_gT\left[\frac{c_0}{WR}ln\left(\frac{c_b}{c_0}\right) - c_d ln\left(\frac{c_b}{c_d}\right)\right] \tag{3}$$

where c_0, c_d, and c_b are the salinity of the feed, the diluate, and the brine streams (mol m^{-3}), respectively, R_g is the gas constant, T is the absolute temperature, and *WR* is the water recovery (defined in the following subsection 2.3).

For membrane-based separation processes, the desalination rate is often quantified as the volumetric flowrate of the product water per unit area of membrane, which is termed as productivity. Thus, the productivity (P) is calculated as follows:

$$P = \frac{Q_d}{A_m} \tag{4}$$

where A_m is the projected area of a single ion-exchange membrane. We reiterate that both performance metrics, *SEC* and P, must be considered simultaneously to effectively evaluate the desalination performance. The removal of salt at a faster rate inherently requires a larger amount of energy consumption, making the process less energy efficient. Such interdependence between *SEC* and P, and the tradeoff between *TEE* and P, have been theoretically and experimentally studied for other desalination processes [32,37–39], but have yet to be thoroughly discussed for electrodialysis.

2.3. Desalination parameters

The energy consumption of desalination is dictated by the separation parameters, namely the feed salinity, salt removal, and water recovery. Hence, to predict the *SEC* of ED across the brackish water regime, its dependence on these desalination parameters must be investigated. Here, we employ the conventional definition of salt removal (S_r), in terms of the product water (diluate) salinity and the feed salinity:

$$S_r = 1 - \frac{c_d}{c_0} \tag{5}$$

The water recovery (*WR*) is a measure of the volume of the desalinated water produced per volume of feedwater supplied. It is generally desirable, both from an economic and environmental perspective, to maximize the water recovery. Specifically, increasing *WR* reduces the cost of pretreatment and pumping for a unit volume of diluate, while also reducing the volume of generated brine and associated disposal costs.

For a single-pass ED system, *WR* is given by

$$WR = \frac{Q_d}{Q_{tot}} \tag{6}$$

where Q_{tot} is the total flow rate of the feedwater provided to the cell pair. Note that Q_{tot} is the sum of the flowrate in the diluate channel (Q_d) and the "makeup" feedwater provided to the concentrate channel ($Q_{b,\,f}$). The makeup feedwater is combined with the recirculated concentrate channel effluent ($Q_{b,\,r}$) to equal the flowrate in the concentrate channel (Q_c). The flowrates in adjacent channels are held equal throughout (i.e., $Q_d = Q_c$). A schematic illustration of the feed-and-bleed operation mode is provided in Fig. A1.

3. Mechanistic Nernst-Planck ion transport model

With ED being a relatively mature technology, several distinct approaches have been proposed for its process modeling. However, most models make overarching assumptions or require the use of system-specific empirical relations. Thus, one of the most fundamental and mechanistic methods for the modeling of ED remains the Nernst-Planck based Sonin-Probstein framework, first demonstrated in 1968 and later extended to more accurately describe transport in ion exchange membranes and spacer-filled channels [22,23,28,29]. Such an approach uses

the rigorous solution of the extended Nernst-Planck equation to describe ion flux (J) in terms of advection, diffusion, and electromigration. The extended Nernst-Planck equation applied in two-dimensions is given by [29].

$$J(y) = c(x,y)v(x) - D_d\nabla c(x,y) - D_e z_i c(x,y)\nabla\phi \quad (7)$$

where c is the salt concentration, v is the flow velocity, D_d is the effective diffusion coefficient, D_e is the effective diffusion coefficient for electromigration, z_i is the charge of the salt ion, and ϕ is the dimensionless electrical potential (normalized by the thermal voltage, V_t). At room temperature, the thermal voltage is 0.0256 V. Notably, we do not differentiate the diffusivities of the cation and anion, but rather use a salt (NaCl) diffusion coefficient, as is common in theoretical modeling of electro-driven processes [8,21–23,40]. Application of the Nernst-Planck equation to both the spacer channels and IEMs ultimately allows for the determination of salt concentration and electrical potential at each point of the ED stack [3,22]. In the following sections, we describe the key governing equations used to model the spacer channels and IEMs to highlight the mechanistic approach of the ion-transport model. The detailed derivation of the mechanistic model is provided in the Appendix A.

3.1. Ion transport in the spacer channel

In a conventional plate-and-frame ED stack, feedwater flows along the axial direction down the spacer channels, while ions in the feedwater are transported in the radial direction through the ion-exchange membranes. In such two-dimensional modeling, it is commonly assumed that advective effects are only relevant in the y-direction (along the length of the membrane), whereas diffusion and electromigration are the only phenomena responsible for transport of ions in the x-direction. With the additional assumptions of electroneutrality and steady state conditions, the overall salt mass balance in the spacer channels can be expressed by the following partial differential equation [22], which can be solved using numerical methods:

$$D_d\frac{\partial^2 c(x,y)}{\partial x^2} = v(x)\frac{\partial c(x,y)}{\partial y} \quad (8)$$

However, the solution of Eq. (8) is coupled to several additional differential relations and boundary conditions, which are required for relating the salt concentration to the potential drops and distribution of current through the ED cell pair [8,21–23,28]. Furthermore, unless a plug flow velocity profile is assumed, variable flow velocity in the radial direction (i.e., perpendicular to the membrane) further complicates Eq. (8). Thus, the solution of Eq. (8) at each discretized point in the spacer channels becomes computationally intensive and impractical for extensive process modeling. We note that throughout this study, a parabolic flow profile is assumed in the flow channels.

3.2. Ion transport in the ion exchange membranes

A key feature of ion transport modeling of ED is the ability to predict the non-ideal selectivity of ion-exchange membranes. Particularly, by applying the Nernst-Planck equation to the IEMs, along with the condition of electroneutrality, co-ion transport through the membranes can be described. Specifically, the total ionic flux (J_{ions}) through the membrane is given as [22]

$$J_{ions}(y) = -D_m\left(\frac{\partial c_{T,m}(x,y)}{\partial x} - \omega X\frac{\partial \phi_m(x,y)}{\partial x}\right) \quad (9)$$

where D_m is the salt diffusion coefficient in the membrane, $c_{T,m}$ is the sum of the cation and anion concentrations in the membrane, X is the volumetric fixed charge density of the ion-exchange membrane, ω is the sign of the fixed charge groups, and ϕ_m is the dimensionless electric potential in the membrane. The first term on the right-hand side of Eq. (9) considers the counterproductive back-diffusion of ions through the ion-exchange membrane, while the second term is related to electromigrative transport in the membranes. Hence, whereas most ED models require the assumption of a current efficiency or membrane selectivity, the Nernst-Planck ion transport model is able to predict the current efficiency and membrane selectivity by comparing the total ionic flux, which includes the transport of co-ions, to the charge flux (the difference of cationic and anionic fluxes). Such capability is critical for accurately representing the ED process, as the selectivity of IEMs is highly dependent on solution concentration, and thus may vary significantly throughout the desalination process.

4. Development of a correlation equation for predicting specific energy consumption

4.1. Derivation of the energy consumption based on an equivalent circuit

As illustrated by the rigorous Nernst-Planck ion-transport model, accurate representation of the ED process requires the description of several complex phenomena. Nonetheless, the energy consumption of ED is ultimately dependent on the electrical current and voltage through the stack. Thus, to approximate the *SEC* of ED, we can apply a simple electrical circuit analogy wherein the ED cell is represented by a resistor:

$$SEC = \frac{\bar{I}^2 R}{Q_d} \quad (10)$$

where $\bar{I}$ is the spatially averaged current (A), R is the resistance of an individual cell pair in the ED stack (Ω), and Q_d is the volumetric flowrate of the diluate (product) stream ($m^3\ s^{-1}$) through a single channel.

To calculate the current ($\bar{I}$) in Eq. (10), the amount of transferred charge (q) (C) must first be determined. The transferred charge is dependent on the amount of salt removed and the overall selectivity of the IEMs (S):

$$q = \frac{c_0 S_r Q_d t_d F}{S} \quad (11)$$

where c_0 is the feed salt concentration (mol m^{-3}), S_r is the salt removal, t_d is the duration of the desalination process (s), and F is the Faraday constant (C mol^{-1}). The selectivity (S) is the portion of the transferred charge that is utilized towards the removal of salt. In reality, S is always less than unity due to Faradaic reactions and co-ion transport through the IEMs. We note that the selectivity of the IEMs is inherently variable throughout the desalination process, changing along with the salinities of the diluate and concentrate solutions. However, for the purpose of maintaining simplicity, we consider S to be a fixed value in Eq. (11), representing the average selectivity during the desalination process. The average current can thus be calculated by

$$\bar{I} = \frac{q}{t_d} = \frac{c_0 S_r\ Q_d\ F}{S} \quad (12)$$

In a well-designed ED stack, the overall electrical resistance is largely due to the solution resistance of the ion-depleted diluate stream [41–43]. Accordingly, the cell pair resistance in Eq. (10), R, can be approximated as the diluate solution resistance and can be expressed as

$$R = \frac{L_{sp} V_t}{2 D_e F c_d A_m} \quad (13)$$

where L_{sp} is the spacer thickness (m), D_e is the diffusion coefficient for electromigration ($m^2\ s^{-1}$), c_d is the concentration of the diluate stream (mol m^{-3}), A_m is the projected area of a single IEM (m^2), and V_t is the thermal voltage (i.e., 0.0256 V at room temperature).

By substituting Eqs. (12) and (13) into Eq. (10), the *SEC* can be expressed in terms of the separation conditions and basic system properties:

$$SEC = \left[\frac{c_0 S_r F}{S}\right]^2 \frac{L_{sp} V_t}{2 D_e F c_d} \frac{Q_d}{A_m} \tag{14a}$$

The last factor on the right-hand-side of the equation (Q_d/A_m) is equal to the productivity (P), which as previously discussed in Eq. (4), is an additional key performance metric in evaluating the ED process. Recalling the definition of salt removal, S_r (Eq. (5)), the expression for SEC can be further simplified to

$$SEC = \frac{V_t F}{2 D_e} \frac{c_0 {S_r}^2 L_{sp}}{1 - S_r} \frac{1}{S^2} P \tag{14b}$$

We note that the first factor on the right-hand-side of the equation is a combination of all the constants. We define the second term on the RHS as the salt loading parameter (j_{st}) (mol m^{-2}), which encompasses the desalination conditions and system geometry:

$$j_{st} = \frac{c_0 {S_r}^2 L_{sp}}{1 - S_r} \tag{15}$$

Intuitively, the salt loading parameter increases if the desalination process achieves a more extensive separation (e.g., higher salt removal or treatment of a higher feed concentration). Eq. (14a) can thus be expressed as

$$SEC = \frac{V_t F}{2 D_e} j_{st} \frac{1}{S^2} P \tag{16}$$

4.2. Development of correlation equation

For a given separation, all the variables in Eq. (16) are known except the selectivity of the ion-exchange membranes (S). The selectivity of an ion-exchange membrane (for the exclusive transport of counter-ions) is primarily a function of the membrane's fixed charge and the concentrations of the adjacent solutions. Whereas higher fixed charge densities (X) amplify Donnan exclusion of co-ions, higher salinities screen the membrane charge and diminish selectivity. Hence, for moderate separation (i.e., salt removal and water recovery) of a low concentration feed ($< \sim 3$ g L^{-1}), the selectivity is expected to be near unity. However, for the treatment of higher feed salinities ($> \sim 5$ g L^{-1}) and large extents of water-salt separation, the selectivity is significantly reduced.

With the selectivity of an IEM being dependent on the concentrations of the solutions in contact with it (which inherently change along the length of the membrane), obtaining an analytical expression for the IEM selectivity in ED is very challenging. For deriving a correlation equation, we utilize a simplified selectivity parameter (S_p), which is directly proportional to the selectivity:

$$S_p = \frac{X^m}{c_b + c_d} \propto S \tag{17}$$

where X is the volumetric fixed charge density of the IEM (mol m^{-3}), m is an empirical fitting parameter, and c_b and c_d are the salt concentrations of the brine and diluate streams, respectively (mol m^{-3}). This selectivity parameter captures the dependence of IEM selectivity on the membrane charge and solution concentration. For a targeted separation with a set of predetermined desalination parameters, c_d is related to the feed salinity and salt removal via Eq. (5), and c_b is related to the water recovery (WR) by

$$c_b = \frac{c_0 - c_d(WR)}{1 - WR} \tag{18}$$

Overall, Eq. (16) predicts the SEC of ED for a specified selectivity, productivity, and set of desalination conditions based on a simple electrical circuit. Though our analysis thus far has considered each variable to independently and directly affect the SEC, it is important to note that many of these parameters are actually interdependent, and thus also have an indirect effect on the SEC. For instance, the productivity in ED is controlled by adjusting the flowrate in the spacer channels, which is accounted for in Eq. (16). However, changing the flowrate affects the flow velocity in the channel and thus also impacts the severity of concentration polarization, which determines the concentrations at the two sides of the IEM. In effect, varying the productivity in ED influences the membrane selectivity, introducing additional complexity that is not accounted for in the prediction of SEC by Eq. (16).

Given the shortcomings of Eq. (16), we introduce a power law correlation equation for SEC (kWh m^{-3}). The correlation equation further builds on Eq. (16) by adding fitting power coefficients α, β, and γ to the salt loading parameter (j_{st}), selectivity parameter (S_p), and the productivity (P), respectively:

$$SEC = C {j_{st}}^{\alpha} {S_p}^{\beta} P^{\gamma} \tag{19}$$

We note that in Eq. (19), SEC is the specific energy consumption in units of kWh m^{-3}, P is the productivity in units of L m^{-2} h^{-1}, and C is a coefficient that originates from the constants in Eq. (16) combined with an additional fitting constant.

In Table 1, we summarize each of the parameters in Eq. (19), along with the corresponding units necessary for use of the correlation

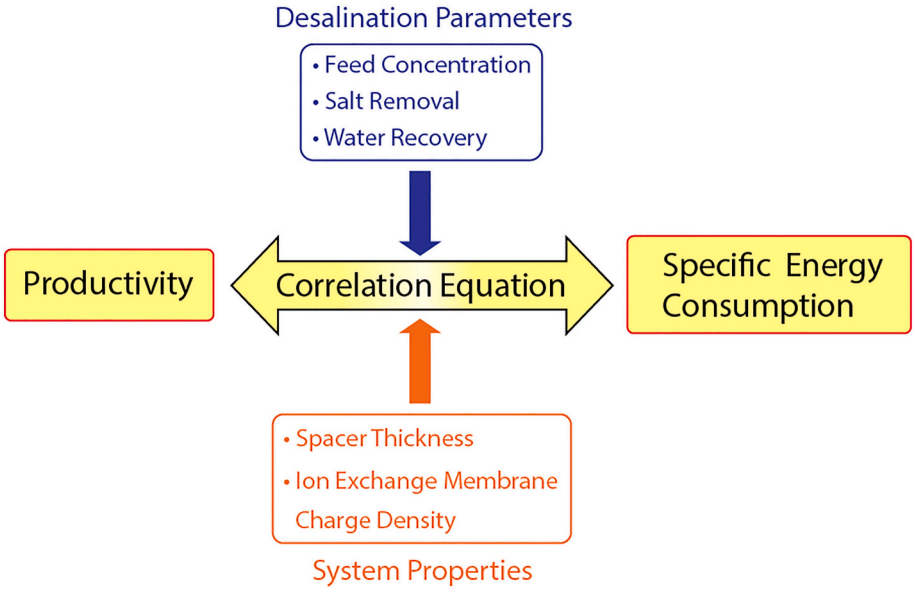

Fig. 2. Schematic description of the process by which the productivity (P) and the specific energy consumption (SEC) are correlated to specified desalination parameters and system properties. The feed concentration (c_0), salt removal (S_r), and water recovery (WR) must be specified to set the desalination parameters (conditions). The correlation equation also requires the input of system properties, particularly the spacer thickness (L_{sp}) and fixed volumetric charge density of the ion exchange membrane (X). Upon providing the inputs, the correlation equation can be used to predict the relationship between the productivity and specific energy consumption.

equation. The coefficients in Eq. (19) are determined by multiple regression fitting with *SEC* values calculated by the numerical ion transport model over a wide range of desalination conditions and system properties (as summarized in Table 2). The multivariable regression is conducted with MATLAB to obtain the values of the coefficients (Table 3). Accordingly, the final form of the correlation equation is given by

$$SEC = 0.091 j_{st}^{\ 0.517} S_p^{\ -0.966} P^{0.281} \quad (20)$$

For a given set of desalination parameters and system properties, Eq. (20) can be utilized to determine the specific energy consumption (for a specified productivity) or the productivity which can be achieved (for a fixed amount of energy), as illustrated by Fig. 2. A spreadsheet for calculating *SEC* based on Eq. (20) is provided as Appendix B. The accuracy of the correlation equation in such application is evaluated in the following section.

5. Correlation equation validation and application

5.1. Comparison of correlation equation with the mechanistic ion-transport model

To validate the accuracy of the correlation equation, we begin by comparing the correlation-predicted *SEC* to the numerical solution of the mechanistic ion transport model (Fig. 3). We perform this comparative assessment over a broad range of desalination conditions (Table 2) to investigate the robustness of the correlation equation. The effects of each of the three desalination parameters (i.e., c_0, S_r, and *WR*) are evaluated by adjusting one variable at a time.

As shown in Fig. 3, the predicted *SEC* by the correlation equation shows remarkable agreement with the ion transport model over nearly all investigated conditions. These results indicate that the simple correlation equation can serve as a reliable substitute for the computationally intensive ion transport model for determination of *SEC*. Notably, the correlation equation shows excellent capability in predicting the energy consumption of ED over a wide range of salt removals, water recoveries, productivities, and membrane charge densities (Fig. 3). We note that the largest discrepancy between the correlation equation and the numerical solution occurs at a productivity of approximately 40 L m^{-2} h^{-1} with an S_r of 70% (Fig. 3C). However, even in this case, the predicted *SEC* by the correlation equation is only 6% smaller than that of the rigorous ion transport model, a relatively small difference for most process modeling purposes.

The trends of the *SEC* are intuitive and align well with those shown in previous studies [3]. For example, for a fixed *WR* (80%) and productivity (20 L m^{-2} h^{-1}), increasing S_r or c_0 requires greater energy consumption. Alternatively, for a fixed S_r and *WR*, increasing c_0 increases the *SEC*. Furthermore, from Fig. 3A, it is apparent that desalination of relatively high c_0 (e.g., 10 g L^{-1}) drastically increases the *SEC* at high S_r, while the *SEC* is relatively insensitive to S_r for c_0 in the lower end of the brackish water regime (e.g., 2 g L^{-1}).

With high *WR* being a key advantage of ED compared to other membrane-based technologies [7,44], we only evaluate *WR* values greater than 50% (Fig. 3B). To achieve a *WR* above 50%, while still maintaining equal flowrate through the diluate and concentrate channels, the "feed-and-bleed" operation mode (Fig. 1) is utilized. In feed-and-bleed operation, a portion of the brine stream is recycled to the concentrate channels, effectively reducing the volume of brackish feedwater supplied per unit of freshwater produced. Though increasing the brine recycle stream flow rate increases the water recovery, it also raises the salinity in the concentrate channels. Thus, a larger concentration (and electrochemical potential) difference is established across the IEMs, which intrinsically requires the application of a larger voltage to transport ions from the diluate to concentrate channel. In addition, the increased transmembrane concentration gradient provides greater driving force for back-diffusion and co-ion transport through the IEM, which is detrimental to the selectivity. For a given separation, this decreased IEM selectivity requires the transport of more counterions across the membranes (i.e., larger current), thereby also requiring a higher applied voltage and *SEC*. As shown by the extremely good match between the correlation equation and the mechanistic model in Fig. 3B, the correlation equation effectively captures the complexities underlying adjustment of the water recovery.

Though analysis of other desalination processes has shown that the specific energy consumption is proportional to the productivity [37,45], such a relation has yet to be systematically demonstrated for electrodialysis. Hence, here we evaluate the relationship between *SEC* and *P* for ED using both the correlation equation and the mechanistic ion transport model (Fig. 3C). The obtained trends for *SEC* as a function of *P* agree very well among both approaches except the small deviation (~6%) near a productivity of 40 L m^{-2} h^{-1} and a salt removal of 70%. A larger productivity decreases the hydraulic residence time of the ions in the flow channels, thus requiring a greater current density and voltage to maintain a fixed S_r. However, for a relatively small S_r (e.g., 30%), increasing *P* shows marginal effects on the *SEC*.

A key property of the IEM which affects the performance of electrodialysis is the membrane fixed charge density. The membrane charge is responsible for the Donnan exclusion of co-ions; thus, a high fixed charge density theoretically enhances the selectivity and efficiency of desalination. However, as shown in Fig. 3D, the relative energetic advantage of increasing fixed charge density strongly depends on the feed salinity. Particularly, membranes with high fixed charge density only provide a substantial reduction of energy consumption for the treatment of higher feed salinities. Increasing the membrane fixed charge density for lower feed salinities ($< \sim 5$ g L^{-1}) has minimal impact on process performance since the selectivity of the IEMs at such salt concentrations is already reasonably close to unity, leaving marginal room for improvement.

5.2. Comparison with literature-reported data

We further validate the correlation equation by comparing its prediction of *SEC* with literature-reported data (Fig. 4). Specifically, we gather experimental and simulation data for steady state ED operation only. However, we note that only a limited number of ED studies have operated under such conditions, making the available data sets scarce. We successfully extract data from four publications: one study aimed at developing a computational program for steady state ED [46], and four well-controlled experimental studies [18,21,47]. The correlation equation requires the input of the desalination parameters and the system properties, each of which are reported in the literature, with the exception of the membrane charge density. Therefore, the membrane charge density is used as a fitting parameter (allowed to vary within a reasonable range), to calculate *SEC* based on the correlation equation. Notably, we use the same membrane charge density for all experiments reported within a single study. In the Appendix A, we summarize the extracted literature data, and the determined charge densities (Table A2). Overall, the correlation equation shows very good agreement with the literature-reported data, demonstrating its robustness in predicting actual ED operation. We note that because the coefficients of the correlation equation are obtained by fitting Eq. (19) with the numerical results of the rigorous ion transport model, the accuracy of the correlation equation is subject to that of the mechanistic model.

5.3. Performance evaluation using the correlation equation

A systematic performance analysis typically entails varying *P* and calculating the corresponding *SEC*, such that one can plot *SEC* vs *P*. Note that for such curves which relate *SEC* and *P*, the separation parameters (i.e., salt removal, water recovery, and feed salinity) must be held constant. As discussed in our previous publications, the absolute value of

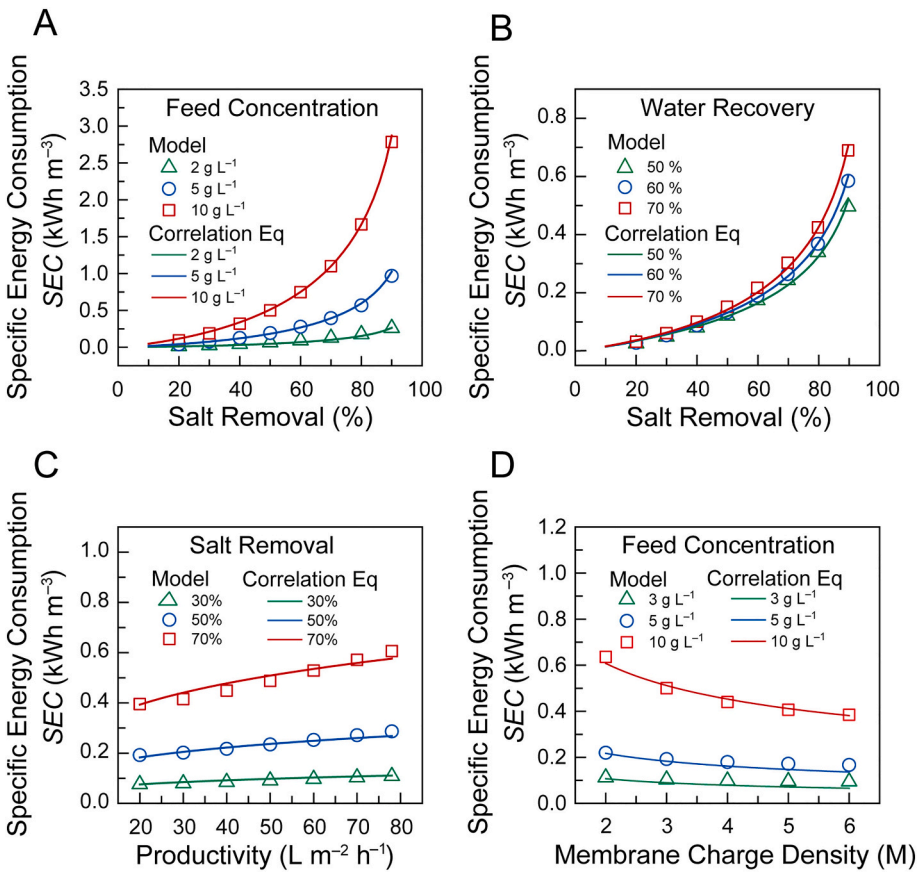

Fig. 3. Comparison of the specific energy consumption (*SEC*) predicted by the correlation equation (solid curves) and the mechanistic ion transport model (open symbols). (A) *SEC* as a function of salt removal for different feed concentrations: 2, 5, and 10 g L^{-1}. The water recovery and productivity are fixed at 80% and 20 L m^{-2} h^{-1}, respectively. (B) *SEC* as a function of salt removal for different water recoveries: 50%, 60%, and 70%. The feed salinity and productivity are fixed at 5 g L^{-1}, and 20 L m^{-2} h^{-1}, respectively. (C) *SEC* as a function of productivity for different salt removals: 30%, 50%, and 70%. The feed salinity and water recovery are fixed at 5 g L^{-1} and 80%, respectively. (D) *SEC* as a function of membrane volumetric charge density (M) at different feed concentrations: 3, 5, and 10 g L^{-1}. The salt removal and water recovery are fixed at 50% and 80%, respectively.

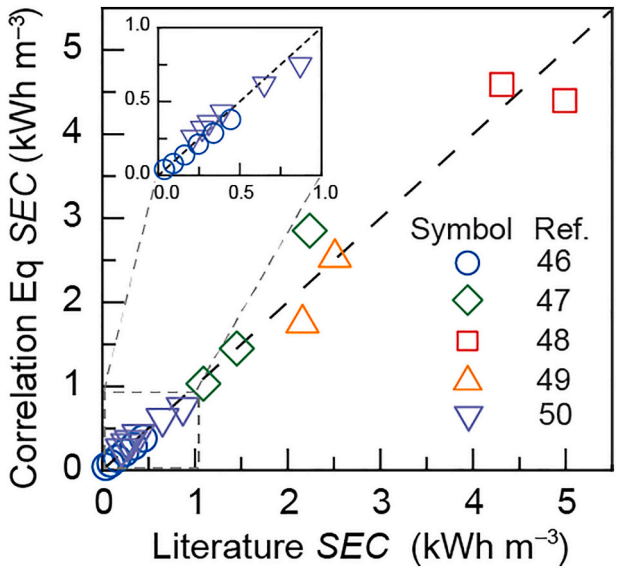

Fig. 4. Comparison between the *SEC* calculated by the correlation equation and reported *SEC* in the literature [46–50]. The desalination parameters and spacer thickness reported in each of the studies are used as the inputs for the correlation equation, while the membrane charge density is an adjusted parameter. The details of the operating conditions are summarized in Table A2 in Appendix A. The dashed line represents ideal match between the correlation equation and the experimental data.

SEC is not relevant without simultaneous consideration of the productivity (i.e., the desalination rate) [31,51]. Thus, a favorable operation would be one which requires a lower *SEC* while achieving the same *P*, or one which achieves a higher *P* for the same *SEC* [32,38]. Typically, such process evaluation is quite complex, requiring intensive computation with a mechanistic model, since the flowrate and the cell voltage must be varied simultaneously to ensure an identical separation. The correlation equation developed in this study, in contrast, predicts the relationship between the *SEC* and *P* in a simple manner, providing an accessible and user-friendly alternative for process design and performance evaluation.

In Fig. 5A, we analyze the performance of ED by employing the correlation equation. As expected, *SEC* monotonically increases with *P*. To desalinate water to a specified effluent concentration, a feed with higher concentration requires more charge transfer across the IEMs, and thereby a larger *SEC*. In addition, from the slopes of the *SEC* vs *P* curves, we observe that *SEC* is more sensitive to *P* when treating a higher salinity feed. This finding suggests that the desalination of feed with low to moderate salinities is favorable for ED, as it can achieve high productivity without incurring a significant energetic penalty.

Though Fig. 5A reveals that the *SEC* of ED considerably increases for higher feed salinities, it is important to note that desalting of higher feed salinity waters inherently requires more energy (as is apparent in Eq. (3)). Hence, in Fig. 5B we report the thermodynamic energy efficiency (*TEE*) which compares the thermodynamic minimum energy consumption for a separation to the actual *SEC* as defined in Eq. (2) [10,51]. As observed with other desalination processes, a tradeoff between the energy efficiency and productivity is observed in ED. Specifically, increasing the feed concentration leads to a smaller *TEE,* indicating a larger degree of irreversible energy consumption as compared to lower feed salinities. In addition, the *TEE* allows for fair comparison of ED with different desalination technologies. Our calculation demonstrates that the *TEE* of ED exceeds 20% when treating a feed salinity of 3 g L^{-1} to standard drinking water concentration (i.e., 0.5 g L^{-1}), making ED comparable to the state-of-art desalination technology, reverse osmosis.

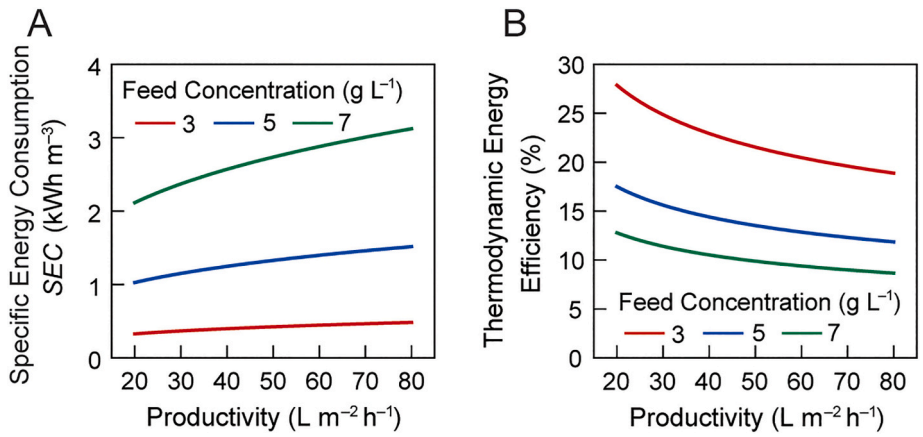

Fig. 5. Performance evaluation of ED for feed concentrations of 3 g L^{-1} (red curve), 5 g L^{-1} (blue curve), and 7 g L^{-1} (green curve). The effluent concentration is fixed at 0.5 g L^{-1}, and the water recovery is 80% throughout. (A) *SEC* increases with productivity for varying feed concentrations, and (B) tradeoff between thermodynamic energy efficiency and productivity for varying feed concentrations.

While a comprehensive evaluation of the two technologies is necessary to draw conclusions on the energetically favorable technology, such analysis is outside the scope of this work. Readers are instead referred to the literature for a recent detailed comparison of the energy efficiency of ED and RO [52].

6. Concluding remarks

Though electrodialysis has been extensively studied for brackish water desalination, mechanistic modeling approaches remain computationally prohibitive as process performance evaluation tools. By using a simple electrical circuit analogue, we derived a mathematically simple, yet reliable correlation equation to calculate the energy consumption of ED. The correlation equation requires the input of the separation parameters (i.e., feed concentration, water recovery and salt removal) and essential system properties (i.e., membrane charge density and spacer channel thickness). To validate the correlation equation, we compared its prediction of *SEC* with that of a 2-D mechanistic ion transport model over a wide range of desalination conditions. The correlation equation was shown to be accurate and robust in its prediction of *SEC*, as demonstrated by its excellent agreement with the *SEC* calculated by the mechanistic model in addition to literature-reported *SEC* data for ED.

In addition, the correlation equation provides an accessible tool for rapid performance analysis of ED. Conventionally, such performance analysis involves evaluating the *SEC* for various separation conditions (i.e., feed salinity, water recovery and salt removal) and productivities. However, with the complex and interconnected transport phenomena of ED, effective performance analysis could until now only be performed through computationally intensive mechanistic modeling. The correlation equation developed in this study effectively relates the two performance metrics — *SEC* and productivity — through a simple relation, providing a facile approach for ED performance analysis. For example, by using the correlation equation, we demonstrated the dependence of *SEC* on productivity and the tradeoff between the thermodynamic energy efficiency and the productivity for the ED process. Therefore, we emphasize that the correlation equation is not only robust in predicting the energy consumption, but also a powerful tool for performance optimization in terms of thermodynamic and kinetic efficiency. Ultimately, we envision that the developed correlation equation will serve as a reliable tool for first-order approximation of ED performance, optimization, and comparison with other desalination technologies.

CRediT authorship contribution statement

Li Wang: Conceptualization, Methodology, Formal analysis, Data curation, Writing – original draft, Writing – review & editing. **Sohum K. Patel**: Methodology, Formal analysis, Writing – original draft, Writing – review & editing. **Menachem Elimelech**: Conceptualization, Supervision, Funding acquisition.

Acknowledgements

We acknowledge the support from the National Science Foundation (NSF) through the Engineering Research for Nanotechnology-Enabled Water Treatment (EEC-1449500) and Grant CBET-2001219.

Appendices. Supplementary data

Supplementary data to this article can be found online at https://doi.org/10.1016/j.desal.2021.115089.

References

[1] E. Jones, M. Qadir, M.T.H. van Vliet, V. Smakhtin, S.M. Kang, The state of desalination and brine production: a global outlook, Sci. Total Environ. 657 (2019) 1343–1356.
[2] V. Pothanamkandathil, J. Fortunato, C.A. Gorski, Electrochemical desalination using intercalating electrode materials: a comparison of energy demands, Environ. Sci. Technol. 54 (2020) 3653–3662.
[3] S.K. Patel, M. Qin, W.S. Walker, M. Elimelech, Energy efficiency of electro-driven brackish water desalination: Electrodialysis significantly outperforms membrane capacitive deionization, Environ. Sci. Technol. 54 (2020) 3663–3677.
[4] L. Wang, S.H. Lin, Theoretical framework for designing a desalination plant based on membrane capacitive deionization, Water Res. 158 (2019) 359–369.
[5] S.K. Patel, C.L. Ritt, A. Deshmukh, Z.X. Wang, M.H. Qin, R. Epsztein, M. Elimelech, The relative insignificance of advanced materials in enhancing the energy efficiency of desalination technologies, Energy Environ. Sci. 13 (2020) 1694–1710.
[6] R. Singh, R. Singh, Chapter 3 - hybrid membrane systems – Applications and case studies, in: Membrane Technology and Engineering for Water Purification, Second edition, Butterworth-Heinemann, Oxford, 2015, pp. 179–281.
[7] A. Campione, L. Gurreri, M. Ciofalo, G. Micale, A. Tamburini, A. Cipollina, Electrodialysis for water desalination: a critical assessment of recent developments on process fundamentals, models and applications, Desalination 434 (2018) 121–160.
[8] H.J. Lee, F. Sarfert, H. Strathmann, S.H. Moon, Designing of an electrodialysis desalination plant, Desalination 142 (2002) 267–286.
[9] S. Al-Amshawee, M.Y.B. Yunus, A.A.M. Azoddein, D.G. Hassell, I.H. Dakhil, H. Abu Hasan, Electrodialysis desalination for water and wastewater: a review, Chem. Eng. J. 380 (2020).
[10] S.H. Lin, Energy efficiency of desalination: fundamental insights from intuitive interpretation, Environ. Sci. Technol. 54 (2020) 76–84.
[11] L. Firdaous, J.P. Maleriat, J.P. Schlumpf, F. Quemeneur, Transfer of monovalent and divalent cations in salt solutions by electrodialysis, Sep. Sci. Technol. 42 (2007) 931–948.

[12] Y.D. Ahdab, D. Rehman, G. Schücking, M. Barbosa, J.H. Lienhard, Treating Irrigation Water Using High-Performance Membranes for Monovalent Selective Electrodialysis, ACS ES&T Water, 2020.
[13] N.P. Berezina, N.A. Kononenko, O.A. Dyomina, N.P. Gnusin, Characterization of ion-exchange membrane materials: properties vs structure, Adv Colloid Interfac 139 (2008) 3–28.
[14] T. Luo, S. Abdu, M. Wessling, Selectivity of ion exchange membranes: a review, J. Membr. Sci. 555 (2018) 429–454.
[15] S.B. Sang, H.L. Huang, Q.M. Wu, An investigation on ion transfer resistance of cation exchange membrane/solution interface, Colloid Surf. A 315 (2008) 98–102.
[16] P. Malek, J.M. Ortiz, H.M.A. Schulte-Herbruggen, Decentralized desalination of brackish water using an electrodialysis system directly powered by wind energy, Desalination 377 (2016) 54–64.
[17] H.M.N. AlMadani, Water desalination by solar powered electrodialysis process, Renew. Energy 28 (2003) 1915–1924.
[18] J.M. Ortiz, J.A. Sotoca, E. Exposito, F. Gallud, V. Garcia-Garcia, V. Montiel, A. Aldaz, Brackish water desalination by electrodialysis: batch recirculation operation modeling, J. Membr. Sci. 252 (2005) 65–75.
[19] M.S. Isaacson, A.A. Sonin, Sherwood number and friction factor correlations for electrodialysis systems, with application to process optimization, Ind. Eng. Chem. Proc. Dd 15 (1976) 313–321.
[20] S. Pawlowski, P. Sistat, J.G. Crespo, S. Velizarov, Mass transfer in reverse electrodialysis: flow entrance effects and diffusion boundary layer thickness, J. Membr. Sci. 471 (2014) 72–83.
[21] N.C. Wright, S.R. Shah, S.E. Amrose, A.G. Winter, A robust model of brackish water electrodialysis desalination with experimental comparison at different size scales, Desalination 443 (2018) 27–43.
[22] M. Tedesco, H.V.M. Hamelers, P.M. Biesheuvel, Nernst-Planck transport theory for (reverse) electrodialysis: I. effect of co-ion transport through the membranes, J. Membr. Sci. 510 (2016) 370–381.
[23] M. Tedesco, H.V.M. Hamelers, P.M. Biesheuvel, Nernst-Planck transport theory for (reverse) electrodialysis: II. Effect of water transport through ion-exchange membranes, J. Membr. Sci. 531 (2017) 172–182.
[24] C.X. Jiang, Q.Y. Wang, Y. Li, Y.M. Wang, T.W. Xu, Water electro-transport with hydrated cations in electrodialysis, Desalination 365 (2015) 204–212.
[25] T. Rottiers, G. De la Marche, B. Van der Bruggen, L. Pinoy, Co-ion fluxes of simple inorganic ions in electrodialysis metathesis and conventional electrodialysis, J. Membr. Sci. 492 (2015) 263–270.
[26] I. Rubinstein, Theory of concentration polarization effects in electrodialysis on counter-ion selectivity of ion-exchange membranes with differing counter-ion distribution coefficients, J. Chem. Soc. Faraday Trans. 86 (1990) 1857–1861.
[27] Y. Tanaka, Concentration polarization in ion-exchange membrane electrodialysis - the events arising in an unforced flowing solution in a desalting cell, J. Membr. Sci. 244 (2004) 1–16.
[28] M. Tedesco, H.V.M. Hamelers, P.M. Biesheuvel, Nernst-Planck transport theory for (reverse) electrodialysis: III. Optimal membrane thickness for enhanced process performance, J. Membr. Sci. 565 (2018) 480–487.
[29] A.A. Sonin, R.F. Probstein, A hydrodynamic theory of desalination by electrodialysis, Desalination 5 (1968) 293.
[30] L. Wang, C.Y. Zhang, C. He, T.D. Waite, S.H. Lin, Equivalent film-electrode model for flow-electrode capacitive deionization: experimental validation and performance analysis, Water Res. 181 (2020).
[31] L. Wang, S.H. Lin, Membrane capacitive deionization with constant current vs constant voltage charging: which is better? Environ. Sci. Technol. 52 (2018) 4051–4060.
[32] H.X. Lu, L. Wang, R. Wycisk, P.N. Pintauro, S.H. Lin, Quantifying the kinetics-energetics performance tradeoff in bipolar membrane electrodialysis, J. Membr. Sci. 612 (2020).
[33] J. Veerman, Reverse electrodialysis: co- and counterflow optimization of multistage configurations for maximum energy efficiency, Membranes-Basel 10 (2020).
[34] L. Gurreri, A. Tamburini, A. Cipollina, G. Micale, Electrodialysis applications in wastewater treatment for environmental protection and resources recovery: a, Syst. Rev. Prog. Perspect. Membrane-Basel 10 (2020).
[35] Y. Tanaka, A computer simulation of feed and bleed ion exchange membrane electrodialysis for desalination of saline water, Desalination 254 (2010) 99–107.
[36] L. Wang, C. Violet, R.M. DuChanois, M. Elimelech, Derivation of the theoretical minimum energy of separation of desalination processes, J. Chem. Educ. 97 (2020) 4361–4369.
[37] S.H. Lin, M. Elimelech, Kinetics and energetics trade-off in reverse osmosis desalination with different configurations, Desalination 401 (2017) 42–52.
[38] L. Wang, S.H. Lin, Intrinsic tradeoff between kinetic and energetic efficiencies in membrane capacitive deionization, Water Res. 129 (2018) 394–401.
[39] Q. Chen, B. Muhammad, F.H. Akhtar, D. Ybyraiymkul, W.S. Muhammad, Y. Li, K. C. Ng, Thermo-economic analysis and optimization of a vacuum multi-effect membrane distillation system, Desalination 483 (2020).
[40] R.K. McGovern, S.M. Zubair, V.J.H. Lienhard, The benefits of hybridising electrodialysis with reverse osmosis, J. Membr. Sci. 469 (2014) 326–335.
[41] P. Dlugolecki, A. Gambier, K. Nijmeijer, M. Wessling, Practical potential of reverse electrodialysis as process for sustainable energy generation, Environ. Sci. Technol. 43 (2009) 6888–6894.
[42] D.A. Vermaas, M. Saakes, K. Nijmeijer, Doubled power density from salinity gradients at reduced intermembrane distance, Environ. Sci. Technol. 45 (2011) 7089–7095.
[43] N.Y. Yip, D.A. Vermaas, K. Nijmeijer, M. Elimelech, Thermodynamic, Energy efficiency, and power density analysis of reverse electrodialysis power generation with natural salinity gradients, Environ. Sci. Technol., 48 (2014) 4925–4936.
[44] H. Strathmann, Ion-Exchange Membrane Separation Processes, Elsevier Science, 2004.
[45] S.A. Hawks, A. Ramachandran, S. Porada, P.G. Campbell, M.E. Suss, P. M. Biesheuvel, J.G. Santiago, M. Stadermann, Performance metrics for the objective assessment of capacitive deionization systems, Water Res. (2018) 152.
[46] Y. Tanaka, Saline water desalination with single-pass ion-exchange membrane electrodialysis - computer simulation, Int. J. Comput. Softw. Eng. 1 (2016) 10.
[47] S.R. Shah, Cost-optimal design of a household batch electrodialysis desalination device, in: Mechanical Engineering, Massachusetts Institute of Technology, 2017.
[48] A.H. Galama, M. Saakes, H. Bruning, H.H.M. Rijnaarts, J.W. Post, Seawater predesalination with electrodialysis, Desalination 342 (2014) 61–69.
[49] A. Gonzalez, M. Grageda, S. Ushak, Assessment of pilot-scale water purification module with electrodialysis technology and solar energy, Appl. Energy 206 (2017) 1643–1652.
[50] G.J. Doornbusch, M. Tedesco, J.W. Post, Z. Borneman, K. Nijmeijer, Experimental investigation of multistage electrodialysis for seawater desalination, Desalination 464 (2019) 105–114.
[51] L. Wang, J.E. Dykstra, S.H. Lin, Energy efficiency of capacitive deionization, Environ. Sci. Technol. 53 (2019) 3366–3378.
[52] S.K. Patel, P.M. Biesheuvel, M. Elimelech, Energy Consumption of Brackish Water Desalination: Identifying the Sweet Spots for Electrodialysis and Reverse Osmosis, ACS ES&T Engineering, 2021.